

Experimental simulation of quantum graphs by microwave networks - Closed and open systems

Michał Ławniczak, Oleh Hul, Szymon Bauch, and Leszek Sirko

Institute of Physics, Polish Academy of Sciences, Aleja Lotników 32/46, 02-668
Warszawa, Poland
(E-mail: sirko@ifpan.edu.pl)

Abstract. We show that chaotic quantum graphs of connected one-dimensional wires can be experimentally simulated by irregular microwave networks consisting of coaxial cables. The spectra of the microwave networks are measured for undirected and directed networks. The directed networks simulating quantum graphs with broken time reversal symmetry consist of microwave circulators apart from coaxial cables. In this way the properties of the graphs such as the nearest neighbor spacing distribution and the lengths of periodic orbits are obtained. Furthermore, we present the results of numerical studies of the parametric level correlation function $c(x)$ for Neumann and circular orthogonal ensemble (COE) graphs. We also demonstrate that microwave networks with absorption can be used to investigate properties of open quantum systems which recently have been extensively studied in the context of transparent electronics and new biosensors. We report the experimental studies of the distributions of Wigner's reaction K matrix for the networks with preserved time reversal symmetry. Moreover, the enhancement factor for the networks simulating open quantum graphs with preserved and broken time reversal symmetry is experimentally evaluated. We demonstrate that the experimental results are in good agreement with the random matrix theory predictions.

Keywords: Microwave networks, Quantum graphs, Random matrix theory.

1 Introduction

Quantum graphs of connected one-dimensional quantum wires were introduced more than seventy years ago by Pauling [1]. The same idea was used later by Kuhn [2] to describe organic molecules by free electron models. Quantum graphs can be considered as idealizations of physical networks in the limit where the widths of the wires are much smaller than their lengths, i.e. assuming that the propagating waves remain in a single transversal mode. Among the systems successfully modeled by quantum graphs one can find e.g., electromagnetic optical waveguides [3,4], mesoscopic systems [5,6], quantum wires [7,8] and excitation of fractons in fractal structures [9,10]. Recently it has been shown that quantum graphs are excellent paradigms of quantum chaos [11–23]. More realistic open systems - microwave networks with moderate and

strong absorption strength $\gamma = 2\pi\Gamma/\Delta$, where Γ is the absorption width and Δ is the mean level spacing, have been experimentally investigated in [24–28]. The distribution of the reflection coefficient $P(R)$ and the distributions of the Wigner reaction matrix [29] (in the literature often called K matrix [30]) for networks (graphs) with time reversal symmetry (TRS) (symmetry class of random matrix theory $\beta = 1$ [31]) in the presence of moderate ($\gamma \leq 7.1$) and strong absorption ($\gamma > 20$) have been respectively studied in [24,25] and [26,28]. The results of the experimental study of the two-port scattering matrix \hat{S} elastic enhancement factor $W_{S,\beta}$ for microwave irregular networks simulating quantum graphs with preserved and broken time reversal symmetry in the presence of absorption was reported in [27,28]. Other interesting open objects - quantum graphs with leads - have been analyzed in details in [14,15].

The paper [21] showed that using a simple experimental setup consisting of microwave networks (throughout the text we also use the names: microwave graphs or circuits) one may successfully simulate quantum graphs. The circuits are constructed of coaxial cables connected by microwave joints. Furthermore, to mimic the effects of the time reversal symmetry breaking in quantum systems it is sufficient to add the microwave circulators [27] into the circuits.

The analogy between quantum graphs and microwave networks is based upon the equivalency of the Schrödinger equation describing the quantum system and the telegraph equation describing the ideal microwave circuit. This paper continues the use of microwave spectroscopy to verify wave effects predicted on the basis of quantum physics, which for two-dimensional systems, thin microwave cavity resonators, was pioneered by [32] and further developed by [24,33–43]. The first microwave experiment specifically devoted to study of quantum chaotic scattering was reported in [44]. Later on a similar experimental technique was applied in the observation of resonance trapping in an open microwave cavity [45]. In the case of two dimensions the Schrödinger equation for quantum billiards is equivalent to the Helmholtz equation for microwave cavities of corresponding shape. Three-dimensional chaotic billiards have been also studied experimentally in the microwave frequency domain [46–50] but for these systems there is no direct analogy between the vectorial Helmholtz equation and the Schrödinger equation.

2 The telegraph equation on a microwave network

A general microwave network consists of N vertices connected by bonds e.g., coaxial cables. The coaxial cable consists of an inner conductor of radius r_1 surrounded by a concentric conductor of inner radius r_2 . The space between the inner and the outer conductors is filled with a homogeneous material having the dielectric constant ε . For frequency ν below the onset of the next TE_{11} mode [51], inside a coaxial cable can propagate only the fundamental TEM mode, in the literature often called a Lecher wave.

In order to find propagation of a Lecher wave inside the coaxial cable joining the i -th and the j -th vertex of the microwave graph one can begin with the continuity equation for the charge and the current on the considered cable (bond) [52]

$$\frac{de_{ij}(x,t)}{dt} = -\frac{dJ_{ij}(x,t)}{dx}, \quad (1)$$

where $e_{ij}(x,t)$ and $J_{ij}(x,t)$ are the charge and the current per unit length on the surface of the inner conductor of a coaxial cable.

For the potential difference one can write down

$$U_{ij}(x,t) = V_2^{ij}(x,t) - V_1^{ij}(x,t) = \frac{e_{ij}(x,t)}{\mathcal{C}}, \quad (2)$$

where $V_1^{ij}(x,t)$ and $V_2^{ij}(x,t)$ are the potentials of the inner and the outer conductors of a coaxial cable and \mathcal{C} is the capacitance per unit length of a cable.

Taking the spatial derivative of (2) and assuming that the wave propagating along the cable is monochromatic $e_{ij}(x,t) = e^{-i\omega t}e_{ij}(x)$ and $U_{ij}(x,t) = e^{-i\omega t}U_{ij}(x)$ one can obtain [52]

$$\frac{d}{dx}U_{ij}(x) = -\mathcal{Z}J_{ij}(x), \quad (3)$$

where $\mathcal{Z} = \mathcal{R} - \frac{i\omega\mathcal{L}}{c^2}$. \mathcal{R} and \mathcal{L} denote the resistance and the inductance per unit length, respectively. The angular frequency ω is equal to $2\pi\nu$ and c stands here for the speed of light in a vacuum.

Making use of the equations (1-3) and the definition of \mathcal{Z} for an ideal lossless coaxial cable with the resistance $\mathcal{R} = 0$, one can derive the telegraph equation on the microwave graph

$$\frac{d^2}{dx^2}U_{ij}(x) + \frac{\omega^2\varepsilon}{c^2}U_{ij}(x) = 0, \quad (4)$$

where $\varepsilon = \mathcal{L}\mathcal{C}$ [53].

It can be easily recognized that assuming the correspondence: $\Psi_{ij}(x) \Leftrightarrow U_{ij}(x)$ and $k^2 \Leftrightarrow \frac{\omega^2\varepsilon}{c^2}$, equation (4) is formally equivalent to the one-dimensional Schrödinger equation (with $\hbar = 2m = 1$) on the graph with the magnetic vector potential $A_{ij} = 0$ [12],

$$\frac{d^2}{dx^2}\Psi_{ij}(x) + k^2\Psi_{ij}(x) = 0. \quad (5)$$

3 Integrated nearest neighbor spacing distribution

The equivalence of irregular microwave networks and chaotic quantum graphs with time reversal symmetry was checked in the paper [21]. In the recent paper Ławniczak et al. [27] additionally demonstrated that in order to mimic the effects of the time reversal symmetry breaking in quantum graphs it is sufficient to add the microwave circulators into the circuits. Microwave networks with circulators are also called directed networks. The important measure of systems' chaotic behavior the integrated nearest neighbor spacing (INNS) distribution $I(s)$ was evaluated experimentally for tetrahedral microwave networks

(number of vertices $n = 4$), simulating quantum graphs with time reversal symmetry [21], and hexagon directed networks ($n = 6$) simulating graphs with broken TRS [27]. Figure 1 shows the experimental set-up for measurements of spectra of hexagon directed networks which was used for evaluation of the integrated nearest neighbor spacing distribution $I(s)$.

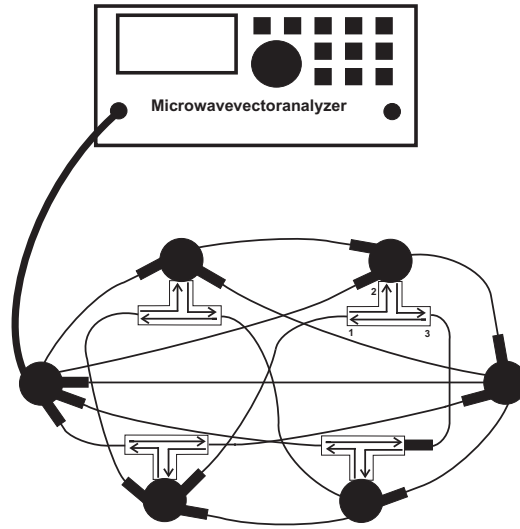


Fig. 1. Experimental set-up for measurements of spectra of hexagon directed networks. In the experiment a vector network analyzer E8364B was used. The full circles and full rectangles represent joints and attenuators, respectively. The arrows in the circulators show directions of signal propagation.

The distribution $I(s)$ is defined as follows

$$I(s) = \int_0^s ds' P(s'), \quad (6)$$

where $P(s')$ [54] is the nearest neighbor spacing distribution.

Figure 2 shows the INNS distribution obtained for tetrahedral microwave networks (number of vertices $n = 4$) simulating quantum graphs with time reversal symmetry. The solid line represents predictions of random matrix theory obtained for Gaussian Orthogonal Ensemble (GOE), applicable for systems with a time-reversal symmetry. The dashed line denotes results characteristic for Gaussian Unitary Ensemble (GUE), used if the time reversal symmetry is broken [54]. Experimental curve (open triangles) was obtained by averaging over the set of 10 microwave graphs obtained by varying the length of one bond, which provided us with the total of 2220 experimentally measured eigenfrequencies. Figure 2 demonstrates that the INNS distribution is in a very good agreement with the GOE prediction.

Figure 2 also shows the INNS distribution obtained for the directed networks. The experimental curve (full circles) obtained by averaging over the

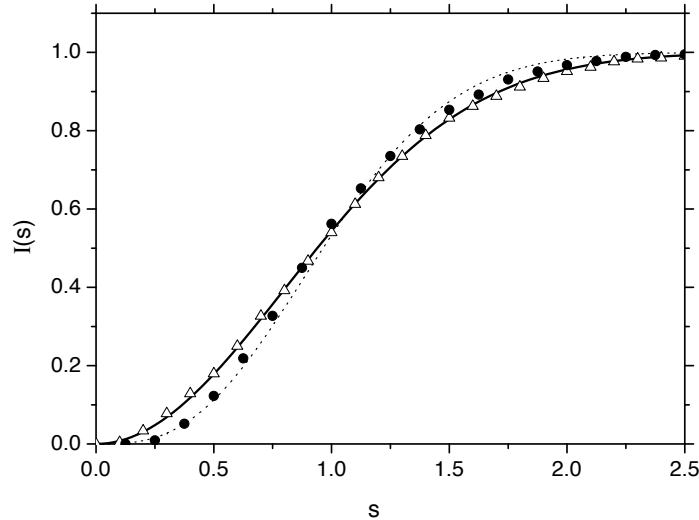


Fig. 2. Integrated nearest neighbor spacing distributions $I(s)$ obtained for tetrahedral networks (open triangles) and hexagon networks (full circles) simulating, respectively, graphs with preserved and broken time reversal symmetry, are compared with the theoretical predictions for GOE (solid line) and GUE (dashed line).

set of 20 directed microwave hexagon networks ($n = 6$) was compared to the predictions of GOE and GUE systems. It is seen that the experimental INNS distribution is in good agreement with the GUE prediction.

4 Lengths of periodic orbits in the network

The measurement of the spectra of the networks enables to calculate the lengths of periodic orbits in the network [21]. They were computed from the Fourier transform

$$F(l) = \int_0^{k_{max}} \tilde{\rho}(k) \omega(k) e^{-ikl} dk, \quad (7)$$

where $\tilde{\rho}$ is the oscillating part of the level density and $\omega(k) = \sin^2(\pi \frac{k}{k_{max}})$ is a window function that suppresses the Gibbs overshoot phenomenon [38,55]. Here k_{max} is the maximal value of the wave number within the interval where the eigenvalues of the network were evaluated. In order to extract the oscillating part of the level density $\tilde{\rho}$ from the density of states $\rho(k) = \sum_j \delta(k - k_j)$ the mean density $\bar{\rho}(k) = d\bar{N}(k)/dk$ was subtracted.

The absolute square of the Fourier transform of the fluctuating part of the density of resonances $|F(l)|^2$ for the network of the “optical” length 223.6 cm is shown in Figure 3. The lengths of the bonds of this network fulfill the following relations: $a < b < c < d < e < f$. Results obtained from the experimental spectrum (solid line) are compared to the results obtained

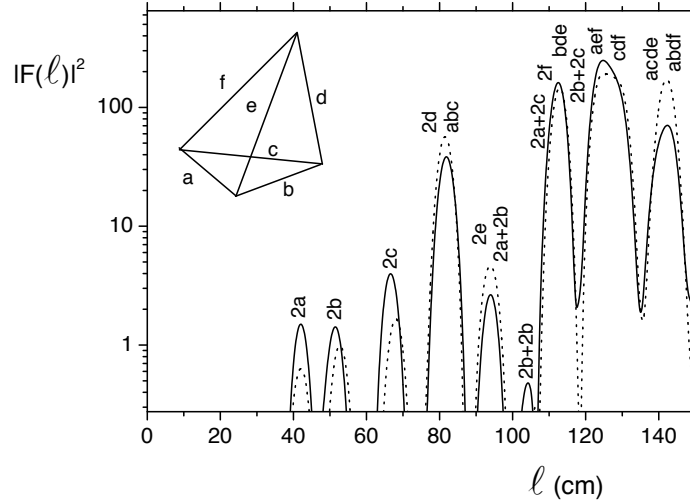


Fig. 3. Absolute square of the Fourier transform of the fluctuating part of the density of resonances of the graph of the “optical” length 223.6 cm. Results of the experiment (solid line) are compared with the numerical results (dotted line). The assignment of peaks of $|F(l)|^2$ to simple periodic orbits is shown along with the length of the orbits. The “optical” lengths of the bonds of the graph: $a = 21.0$ cm, $b = 26.3$ cm, $c = 34.0$ cm, $d = 39.6$ cm, $e = 46.8$ cm, $f = 55.9$ cm.

from numerical calculations (dotted line). The absolute square of the Fourier transform $|F(l)|^2$ shows pronounced peaks near the lengths of periodic orbits. Figure 3 shows good agreement between the experimental and the numerical results.

The above experimental and numerical results clearly show that chaotic quantum graphs can be experimentally simulated by irregular microwave networks consisting of coaxial cables.

5 The autocorrelation function $c(x)$ of the level velocities

Hul et al. [56] demonstrated that for fully connected Neumann graphs (graphs with Neumann boundary conditions at vertices) there are some spectral statistics, e.g., the second order level velocity autocorrelation functions $c(x)$ and $\tilde{c}(\omega, x)$ that for larger graphs ($n > 6$) show deviations from the predictions of RMT for GOE. This important property of large graphs has been further investigated numerically in the recent paper [23] where fully connected Neumann and COE quantum graphs of different size were considered. COE graphs are characterized by the circular orthogonal ensemble boundary conditions. Here, we would like to demonstrate that for larger COE graphs the autocorrelation functions of velocities $c(x)$, in contrast to large Neumann graphs, show very good overall agreement with the random matrix theory predictions.

The autocorrelation function $c(x)$ of the level velocities is defined as follows:

$$c(x) = \left\langle \frac{\partial \xi_i}{\partial \bar{x}}(\bar{x}) \frac{\partial \xi_i}{\partial \bar{x}}(\bar{x} + x) \right\rangle, \quad (8)$$

where ξ_i are the rescaled eigenenergies of the graph, x is the rescaled external parameter X [56]. The average $\langle \dots \rangle$ is performed over the parameter \bar{x} and over all the energy levels. The autocorrelation function $c(x)$ measures the correlation of the level velocities which belong to the same energy level. We chose the change of the bonds lengths of a graph to be the external parameter X . For the graphs with the even number of bonds the lengths of all the bonds were changed, while for the graphs with the odd number of bonds we changed the lengths of all the bonds except the arbitrary chosen one.

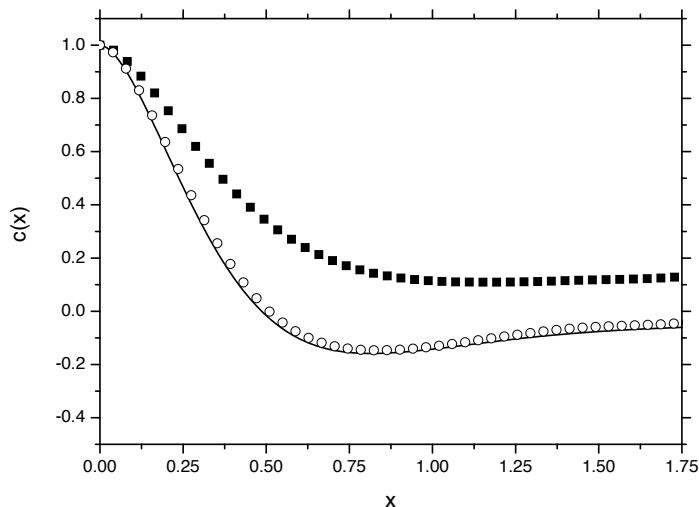


Fig. 4. The velocity autocorrelation function $c(x)$ for Neumann (full squares) and COE (open circles) graphs with $n = 20$ vertices compared to the results of RMT for GOE (solid line).

In Figure 4 we show our recent numerical results for the velocity autocorrelation function $c(x)$ for Neumann (full squares) and COE (open circles) graphs with $n = 20$ vertices compared to the results of RMT for GOE (solid line). It is clearly seen that for large COE graphs with $n = 20$ vertices the velocity autocorrelation function $c(x)$ is very close to the RMT predictions. Oppositely, for Neumann graphs due to the importance of localization effects in graphs [23] a significant departure from the GOE prediction is observable.

6 Microwave networks with absorption

A network with no absorption and no leads to the outside world is a closed system. However, in a real microwave network there exist absorption and/or leads

which create an open system. Absorption in an undirected microwave network (without microwave circulators) and directed networks can be efficiently varied by changing the length of the cables [21] or by adding microwave attenuators [25].

6.1 Distributions of the reflection coefficient R and the Wigner's reaction matrix K

In this paragraph we would like to present the results of experimental study of the distribution $P(R)$ of the reflection coefficient R and the distributions of imaginary and real parts of Wigner's reaction matrix K [29,30] for microwave networks with absorption that correspond to quantum graphs with time reversal symmetry ($\beta = 1$ symmetry class of random matrix theory [31]).

The K matrix and the scattering matrix S are related by

$$S = \frac{1 - iK}{1 + iK}. \quad (9)$$

Additionally, the function $K = -iZ$ and the scattering matrix $S = (1 - Z)/(1 + Z)$ are directly connected with the impedance Z , which has been recently measured in a microwave cavity experiment [57,58].

In the case of systems coupled by a single-channel antenna the scattering matrix S can be parameterized as

$$S = \sqrt{R}e^{i\theta}, \quad (10)$$

where R is the reflection coefficient and θ is the phase.

The properties of statistical distributions of the scattering matrix S with direct processes and imperfect coupling were considered in several important theoretical papers [59–62]. The distribution of the S matrix for chaotic microwave cavities with absorption was also experimentally investigated [63]. The distribution $P(R)$ of the reflection coefficient R has been recently known for any dimensionless absorption strength γ [64] and for systems with time reversal symmetry ($\beta = 1$) $P(R)$ was studied experimentally in [65]. Moreover, in the papers Hul et al. [25] and Lawniczak et al. [26] the distribution $P(R)$ of the reflection coefficient R and the distributions of imaginary and real parts of Wigner's reaction matrix K for microwave networks with absorption were found using the impedance approach [57,58].

Figure 5 shows the experimental distributions $P(R)$ (squares) of the reflection coefficient R for two mean values of the parameter $\bar{\gamma}$, viz., 20.1 and 50.6. The experimental values of the γ parameter were estimated for each realization of the network by adjusting the theoretical mean reflection coefficient $\langle R \rangle_{th}$ to the experimental one $\langle R \rangle = \langle SS^\dagger \rangle$, where

$$\langle R \rangle_{th} = \int_0^1 dR R P(R). \quad (11)$$

Figure 5 also presents the corresponding numerical distributions $P(R)$ (full lines) evaluated on the basis of the accurate formula given in [64]. A good

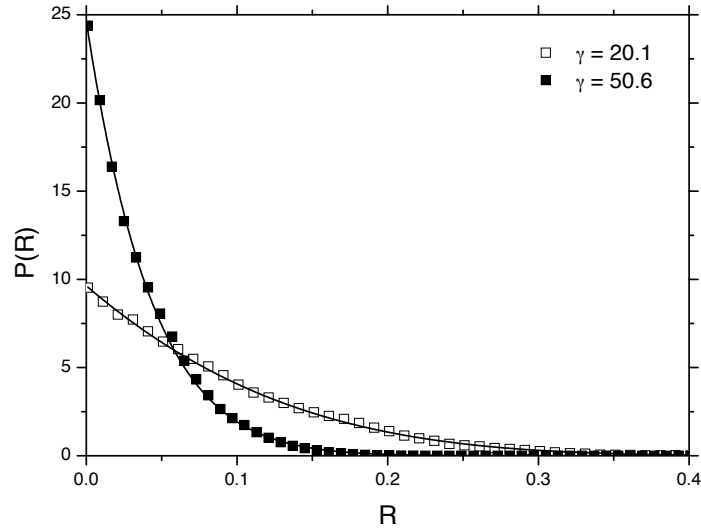


Fig. 5. Experimental distribution $P(R)$ of the reflection coefficient R for the microwave fully connected hexagon networks for $\bar{\gamma} = 20.1$ (open squares) and $\bar{\gamma} = 50.6$ (full squares) [26]. The corresponding theoretical distribution $P(R)$ [64] for $\gamma = 20.1$ and $\gamma = 50.6$, respectively, is marked by the solid line.

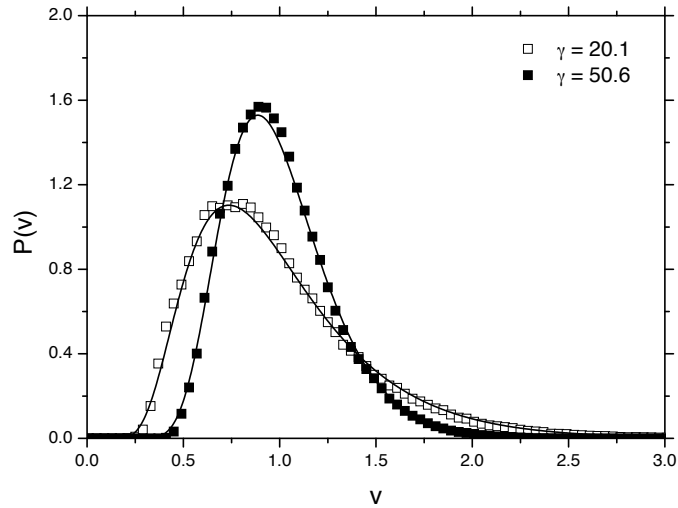


Fig. 6. Experimental distribution $P(v)$ of the imaginary part of the K matrix for the two values of the mean absorption parameter: $\bar{\gamma} = 20.1$ (open squares) and $\bar{\gamma} = 50.6$ (full squares) [26]. The corresponding theoretical distribution $P(v)$ [64] for $\gamma = 20.1$ and $\gamma = 50.6$, respectively, is marked by the solid line.

overall agreement of the experimental distributions $P(R)$ with their theoretical counterparts is seen.

In Figure 6 the experimental distribution $P(v)$ of the imaginary part of the K matrix ($-v = \text{Im } K < 0$) is shown for the two mean values of the parameter $\bar{\gamma} = 20.1$ and 50.6 , respectively. The experimental results in Figure 6 are in general in good agreement with the theoretical ones [26,64]. However, both experimental distributions are slightly higher than the theoretical ones in the vicinity of their maxima.

6.2 Elastic enhancement factor $W_{S,\beta}$

Microwave networks appeared to be very convenient for the experimental studies of the two-port scattering matrix \hat{S} elastic enhancement factor $W_{S,\beta}$ [66,67]. The experiment was performed for microwave irregular networks simulating quantum graphs with preserved and broken time reversal symmetry in the presence of moderate and strong absorption [28]. In the experiment quantum graphs with preserved time reversal symmetry were simulated by microwave networks which were built of attenuators and coaxial cables connected by joints. Absorption in the networks was controlled by the use of microwave attenuators. In order to simulate quantum graphs with broken time reversal symmetry we used the microwave networks with microwave circulators. One should mention that the paper [68] has already reported a weak change of the enhancement factor due to partially broken time invariance in microwave cavity.

In the case of the two-port scattering matrix

$$\hat{S} = \begin{bmatrix} S^{aa} & S^{ab} \\ S^{ba} & S^{bb} \end{bmatrix} \quad (12)$$

the elastic enhancement factor $W_{S,\beta}$ is defined by the following relation [66,67]

$$W_{S,\beta} = \frac{\sqrt{\text{var}(S^{aa})\text{var}(S^{bb})}}{\text{var}(S^{ab})}, \quad (13)$$

where $\text{var}(S^{ab}) \equiv \langle |S^{ab}|^2 \rangle - |\langle S^{ab} \rangle|^2$ denotes the variance of the scattering matrix element S^{ab} . One of the most important property of the enhancement factor $W_{S,\beta}$ for $\gamma \gg 1$ is connected with the fact that it should not depend on the direct processes present in the system [67,69].

In Figure 7 the enhancement factor $W_{S,\beta}$ of the two-port scattering matrix \hat{S} of the microwave networks simulating quantum graphs with preserved and broken TRS, respectively, is shown as a function of the parameter γ .

The experimental results for the networks with preserved TRS (open circles) are in general good agreement with the theoretical ones predicted by [66,67]. Even for moderate absorption the experimental results are close to the theoretical ones. Because of absorption of microwave cables (network bonds) we could not test experimentally predicted by the theory [66,67] increase of the enhancement factor $W_{S,\beta=1} \rightarrow 3$ for very small values of the parameter γ .

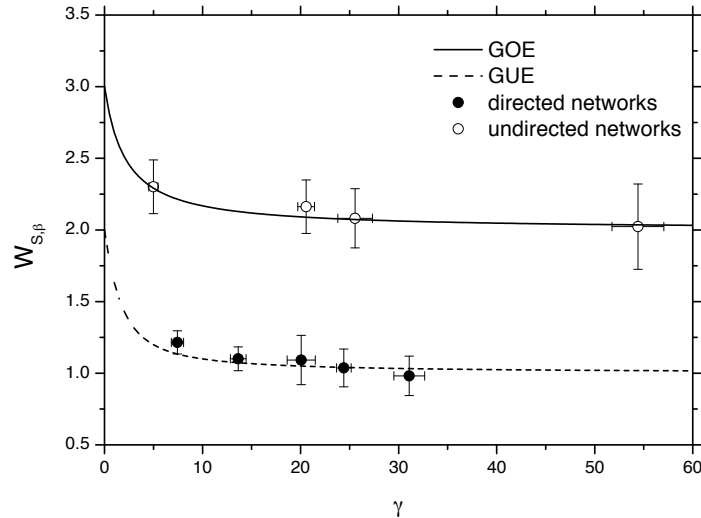


Fig. 7. The enhancement factor $W_{S,\beta}$ of the two-port scattering matrix \hat{S} of the microwave networks simulating quantum graphs with preserved and broken TRS, open circles and full circles respectively, in the function of the parameter γ [28]. The experimental results are compared to the theoretical predictions for GOE (full line) and GUE (broken line).

Figure 7 also shows that in the case of networks with broken TRS in the presence of moderate and strong absorption the experimental results (full circles) are in good agreement with the theoretical ones $W_{S,\beta=2} \simeq 1$ predicted by [66,67,69] within the framework of random matrix theory.

7 Conclusions

We demonstrated that quantum graphs with Neumann boundary conditions can be simulated experimentally by microwave networks. Undirected microwave networks simulate quantum graphs with time reversal symmetry. The results for the directed microwave networks with microwave circulators show that their characteristics such as the integrated nearest neighbor spacing distribution significantly differ from the RMT prediction for GOE, approaching the results characteristic of GUE. Therefore, directed networks can be used to simulate quantum graphs with broken TRS.

We also show that there are some spectral statistics, e.g., the second order level velocity autocorrelation function $c(x)$ that for larger fully connected Neumann graphs show deviations from the predictions of RMT for GOE. These parasite effects of localization can be minimized by use of COE graphs for which the autocorrelation function $c(x)$, in contrast to large Neumann graphs, shows very good overall agreement with the random matrix theory predictions.

Microwave irregular networks consisting of cables and attenuators are also very useful models of experimental systems with absorption. The experimental

results for the distribution $P(R)$ of the reflection coefficient R and the distributions $P(v)$ of the imaginary part of Wigner's reaction matrix obtained for microwave networks with absorption are in good overall agreement with the recent exact theoretical predictions for quantum systems with absorption [64].

The experimental studies of the enhancement factor $W_{S,\beta}$ of the two-port scattering matrix \hat{S} for the microwave networks simulating quantum systems with preserved and broken TRS in the presence of absorption show good agreement with the theoretical predictions.

The results presented in this paper clearly demonstrate that undirected and directed microwave networks which simulate undirected and directed quantum graphs, respectively, can be successfully used to study large variety of wave phenomena predicted by quantum physics.

Acknowledgments. This work was supported by the Ministry of Science and Higher Education grant No. N N202 130239.

References

- 1.L. Pauling, J. Chem. Phys. **4**, 673 (1936).
- 2.H. Kuhn, Helv. Chim. Acta, **31**, 1441 (1948).
- 3.C. Flesia, R. Johnston, and H. Kunz, Europhys. Lett. **3**, 497 (1987).
- 4.R. Mitra and S. W. Lee, *Analytical techniques in the Theory of Guided Waves* (Macmillan, New York, 1971).
- 5.Y. Imry, *Introduction to Mesoscopic Systems* (Oxford, New York, 1996).
- 6.D. Kowal, U. Sivan, O. Entin-Wohlman, Y. Imry, Phys. Rev. B **42**, 9009 (1990).
- 7.E. L. Ivchenko, A. A. Kiselev, JETP Lett. **67**, 43 (1998).
- 8.J.A. Sanchez-Gil, V. Freilikher, I. Yurkevich, and A. A. Maradudin, Phys. Rev. Lett. **80**, 948 (1998).
- 9.Y. Avishai and J.M. Luck, Phys. Rev. B **45**, 1074 (1992).
- 10.T. Nakayama, K. Yakubo, and R. L. Orbach, Rev. Mod. Phys. **66**, 381 (1994).
- 11.T. Kottos and U. Smilansky, Phys. Rev. Lett. **79**, 4794 (1997).
- 12.T. Kottos and U. Smilansky, Annals of Physics **274**, 76 (1999).
- 13.T. Kottos and U. Smilansky, Phys. Rev. Lett. **85**, 968 (2000).
- 14.T. Kottos and H. Schanz, Physica E **9**, 523 (2003).
- 15.T. Kottos and U. Smilansky, J. Phys. A **36**, 3501 (2003).
- 16.F. Barra and P. Gaspard, Journal of Statistical Physics **101**, 283 (2000).
- 17.G. Tanner, J. Phys. A **33**, 3567 (2000).
- 18.P. Pakoński, K. Życzkowski and M. Kuś, J. Phys. A **34**, 9303 (2001).
- 19.P. Pakoński, G. Tanner and K. Życzkowski, J. Stat. Phys. **111**, 1331 (2003).
- 20.R. Blümel, Yu Dabaghian, and R.V. Jensen, Phys. Rev. Lett. **88**, 044101 (2002).
- 21.O. Hul, S. Bauch, P. Pakoński, N. Savytskyy, K. Życzkowski, and L. Sirko, Phys. Rev. E **69**, 056205 (2004).
- 22.O. Hul, M. Ławniczak, S. Bauch, and L. Sirko, Symposia in Pure Mathematics **77**, 595 (2008).
- 23.O. Hul and L. Sirko, Phys. Rev. E **83**, 066204 (2011).
- 24.O. Hul, O. Tymoshchuk, Sz. Bauch, P. M. Koch and L. Sirko, J. Phys. A **38**, 10489 (2005).
- 25.O. Hul, S. Bauch, M. Ławniczak, and L. Sirko, Acta Phys. Pol. A **112**, 655 (2007).
- 26.M. Ławniczak, O. Hul, S. Bauch, P. Šeba, and L. Sirko, Phys. Rev. E **77**, 056210 (2008).

- 27.M. Lawniczak, S. Bauch, O. Hul, and L. Sirko, Phys. Scr. **T135**, 014050 (2009).
- 28.M. Lawniczak, S. Bauch, O. Hul, and L. Sirko, Phys. Rev. E **81**, 046204 (2010).
- 29.G. Akguc and L. E. Reichl, Phys. Rev. E **64**, 056221 (2001).
- 30.Y.V. Fyodorov and D.V. Savin, JETP Letters **80**, 725 (2004).
- 31.M.L. Mehta, *Random matrices*, Third edition, (Elsevier/Academic Press, Amsterdam, 2004).
- 32.H.J. Stöckmann and J. Stein, Phys. Rev. Lett. **64**, 2215 (1990).
- 33.S. Sridhar, Phys. Rev. Lett. **67**, 785 (1991).
- 34.H. Alt, H.-D. Gräf, H. L. Harner, R. Hofferbert, H. Lengeler, A. Richter, P. Schardt, and A. Weidenmüller, Phys. Rev. Lett. **74**, 62 (1995).
- 35.P. So, S. M. Anlage, E. Ott, and R. N. Oerter, Phys. Rev. Lett. **74**, 2662 (1995).
- 36.U. Stöffregen, J. Stein, H.-J. Stöckmann, M. Kuś, and F. Haake, Phys. Rev. Lett. **74**, 2666 (1995).
- 37.F. Haake, M. Kuś, P. Šeba, H.-J. Stöckmann, and U. Stöffregen, J. Phys. A **29**, 5745 (1996).
- 38.L. Sirko, P. M. Koch, and R. Blümel, Phys. Rev. Lett. **78**, 2940 (1997).
- 39.S. Bauch, A. Błędowski, L. Sirko, P. M. Koch, and R. Blümel, Phys. Rev. E **57**, 304 (1998).
- 40.R. Blümel, P. M. Koch, and L. Sirko, Foundation of Physics **31**, 269 (2001).
- 41.L. Sirko, Sz. Bauch, Y. Hlushchuk, P.M. Koch, R. Blmel, M. Barth, U. Kuhl, and H.-J. Stöckmann, Phys. Lett. A **266**, 331-335 (2000).
- 42.N. Savvitsky, A. Kohler, S. Bauch, R. Blümel, and L. Sirko, Phys. Rev. E **64**, 036211 (2001).
- 43.N. Savvitsky, O. Hul, and L. Sirko, Phys. Rev. E **70**, 056209 (2004).
- 44.E. Doron, U. Smilansky, and A. Frenkel, Phys. Rev. Lett. **65**, 3072 (1990).
- 45.E. Persson, I. Rotter, H.-J. Stöckmann, and M. Barth **85**, 2478 (2000).
- 46.O. Tymoshchuk, N. Savvitsky, O. Hul, S. Bauch, and L. Sirko, Phys. Rev. E **75**, 037202 (2007).
- 47.N. Savvitsky, O. Tymoshchuk, O. Hul, S. Bauch, and L. Sirko, Phys. Lett. A **372**, 1851 (2008).
- 48.M. Lawniczak, O. Hul, S. Bauch, and L. Sirko, Acta Phys. Pol. A **116**, 749 (2009).
- 49.S. Deus, P. M. Koch, and L. Sirko, Phys. Rev. E **52**, 1146 (1995).
- 50.C. Dembowski, B. Dietz, H.-D. Gräf, A. Heine, T. Papenbrock, A. Richter, and C. Richter, Phys. Rev. Lett. **89**, 064101-1 (2002).
- 51.D. S. Jones, *Theory of Electromagnetism* (Pergamon Press, Oxford, 1964), p. 254.
- 52.L.D. Landau, E.M. Lifshitz, *Electrodynamics of Continuous Media* (Pergamon Press, Oxford, 1960).
- 53.G. Goubau, *Electromagnetic Waveguides and Cavities* (Pergamon Press, Oxford, 1961).
- 54.F. Haake *Quantum Signatures of Chaos* (II ed. Springer, Berlin, 2000).
- 55.Sz. Bauch, A. Błędowski, L. Sirko, P. M. Koch, and R. Blümel, Phys. Rev. E **57**, 304 (1998).
- 56.O. Hul, P. Šeba, and L. Sirko, Phys. Rev. E **79**, 066204 (2009).
- 57.S. Hemmady, X. Zheng, T.M. Antonsen Jr., E. Ott, and S.M. Anlage, Acta Physica Polonica A **109**, 65 (2006).
- 58.S. Hemmady, X.Zheng, E. Ott, T.M. Antonsen, and S.M. Anlage, Phys. Rev. Lett. **94**, 014102 (2005).
- 59.G. López, P.A. Mello, and T.H. Seligman, Z. Phys. A **302**, 351 (1981).
- 60.E. Doron and U. Smilansky, Nucl. Phys. A **545**, 455 (1992).
- 61.P.W. Brouwer, Phys. Rev. B **51**, 16878 (1995).
- 62.D.V. Savin, Y.V. Fyodorov, and H.-J. Sommers, Phys. Rev. E **63**, 035202 (2001).

63. U. Kuhl, M. Martinez-Mares, R.A. Méndez-Sánchez, and H.-J. Stöckmann, *Phys. Rev. Lett.* **94**, 144101 (2005).
64. D.V. Savin, H.-J. Sommers, and Y.V. Fyodorov, *JETP Letters* **82**, 544 (2005).
65. R.A. Méndez-Sánchez, U. Kuhl, M. Barth, C.V. Lewenkopf, and H.-J. Stöckmann, *Phys. Rev. Lett.* **91**, 174102-1 (2003).
66. Y.V. Fyodorov, D.V. Savin, and H.-J. Sommers, *J. Phys. A* **38**, 10731 (2005).
67. D.V. Savin, Y.V. Fyodorov, and H.-J. Sommers, *Acta Physica Polonica A* **109**, 53 (2005).
68. B. Dietz, T. Friedrich, H. L. Harney, M. Miski-Oglu, A. Richter, F. Schäfer, J. Verbaarschot, and H. A. Weidenmüller, *Phys. Rev. Lett.* **103**, 064101 (2009).
69. X. Zheng, S. Hemmady, T. M. Antonsen, Jr., S. M. Anlage, and E. Ott, *Phys. Rev. E* **73**, 046208 (2006).